

Per-Query Visual Concept Learning

Ori Malca¹ Dvir Samuel^{1,2} Gal Chechik^{1,3}

¹Bar-Ilan University ²OriginAI ³NVIDIA

Project page: <https://per-query-visual-concept-learning.github.io>

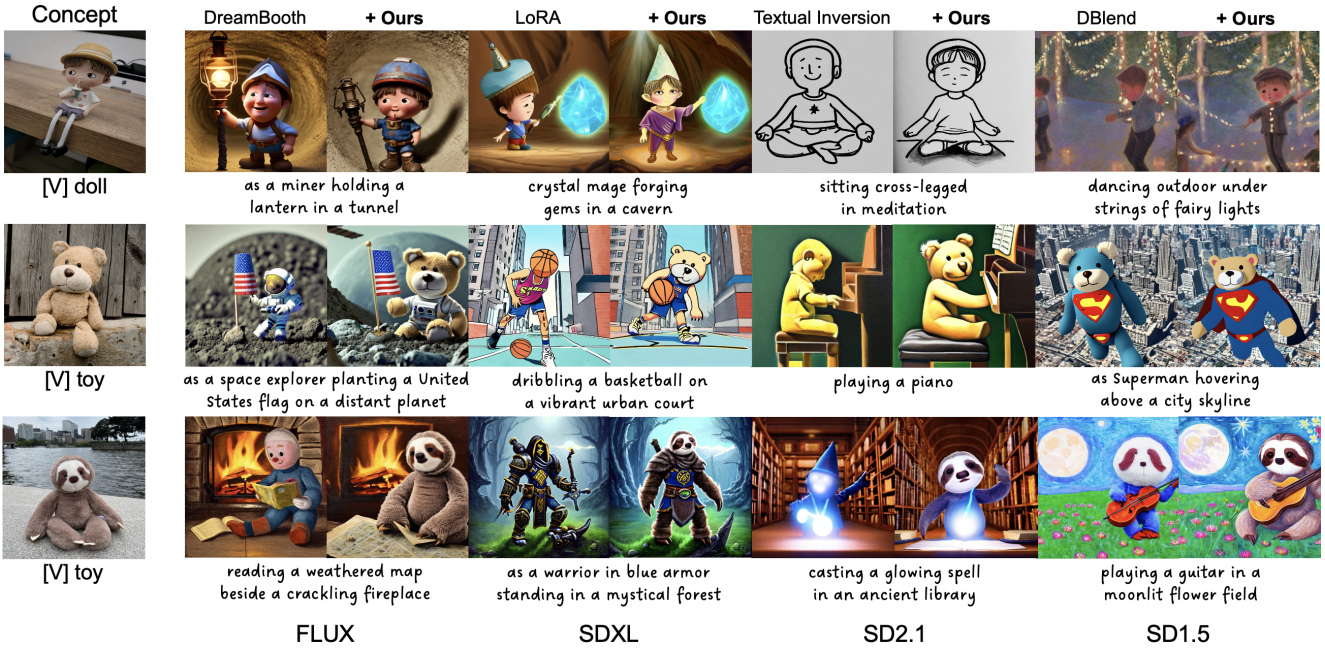


Figure 1. Given a pretrained text-to-image personalization checkpoint, our method enhances per-query generation in terms of image alignment and text alignment, with just a single gradient update (~4 seconds on an NVIDIA H100 GPU). It is compatible with a wide range of personalization techniques (e.g., DreamBooth [26], LoRA [16], Textual Inversion [8], DBLend [22]) and supports various diffusion backbones, including UNet-based models (e.g., SDXL [20], SD [25]) and transformer-based models (e.g., FLUX [13]).

Abstract

Visual concept learning, also known as Text-to-image personalization, is the process of teaching new concepts to a pretrained model. This has numerous applications from product placement to entertainment and personalized design. Here we show that many existing methods can be substantially augmented by adding a personalization step that is (1) specific to the prompt and noise seed, and (2) using two loss terms based on the self- and cross- attention, capturing the identity of the personalized concept. Specifically, we leverage PDM features - previously designed to capture identity - and show how they can be used to improve personalized semantic similarity. We evaluate the benefit

that our method gains on top of six different personalization methods, and several base text-to-image models (both UNet- and DiT-based). We find significant improvements even over previous per-query personalization methods.

1. Introduction

Visual concept learning in generative text-to-image models is the problem of teaching a new concept to a pretrained model [8, 26, 38], usually from a handful of images of the target concept. This process, also known as *personalization*, is typically achieved by tuning small parts of a pre-trained text-to-image model models, like the embedding layer of a

token [8], or a low-rank adaptation of the attention layers (DreamBooth LoRA [16, 26]). Personalization methods are evaluated in two main aspects: How well they capture the visual appearance of the target concept (*image alignment*) and how well it can be controlled to agree with new text prompts (*textual alignment*). While significant progress has been made in this area, significant room is left for further improvement, especially when the number of target concept images that is available for fine-tuning is small.

Here we propose to improve generation of a new visual concept using two observations. First, that the (reconstruction) losses used for personalization were typically not designed for capturing concept identity. Second, that personalization methods typically fine-tune models using a diverse set of prompts and seeds, with the goal of using the learned concept with any seed and prompt at inference time (see [1, 3]). To address this, we introduce a novel loss function tailored to better preserve visual identity. Our approach is inspired by recent work [28], which found that object appearance is largely encoded in specific layers of the self-attention mechanism. These features were originally used for instance retrieval and segmentation, and here we adapt this insight to improve the training process of existing personalization methods. To further improve text-image alignment, we show that fine-tuning with a fixed prompt and seed significantly enhances generation quality.

We describe an "add-on" fine tuning procedure that can be used on top of existing methods. For instance, once a visual concept has been learned using some method, we perform feature extraction to compute identity-sensitive features from the self-attention part, and prompt-sensitive features from the cross-attention part, and update the model using a single gradient update. We find that this single update step provides significant gains in terms of visual alignment and text alignment. The procedure is simple, fast, and easy to implement. We tested it on top of six different personalization methods and backbone text-to-image diffusion models, (both SD [25], SDXL [20] and Flux [13]) and found that it provides consistent gains.

The paper therefore makes the following contributions: **(1)** An identity-preserving loss based on self and cross attention. **(2)** New SoTA results in personalization using a single image of the target concept. **(3)** It demonstrates the benefit of fine-tuning with a specific seed and prompt.

2. Related work

Text-to-image diffusion models are trained to generate samples from a conditional data distribution by progressively denoising a variable initially sampled from a Gaussian distribution. Recent advances in text-to-image synthesis have been driven by large-scale models trained on massive web-sourced datasets [23–25, 27, 30, 37].

Personalization in generative text-to-image models in-

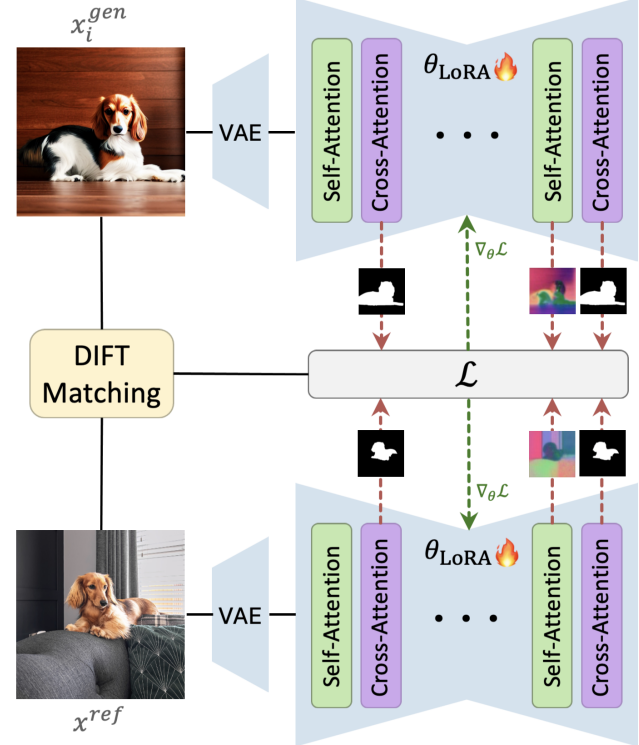


Figure 2. Method Overview. We enhance personalized text-to-image models by computing self- and cross-attention features from a single denoising step of a generated image x^{gen} and a reference image x^{ref} . Using DIFT, we match these features and define losses \mathcal{L}_{SA} , \mathcal{L}_{CA} , and \mathcal{L}_{LDM} , which are combined to update the personalization tuning parameters via gradient descent.

volves teaching a pre-trained model a new concept using only a few images. Early approaches tackled this problem by optimizing word embeddings [2, 8, 33, 35] or fine-tuning model weights [26]. While fine-tuning typically yields better subject fidelity and photorealism—thanks to its higher expressive capacity—it tends to compromise prompt fidelity and image diversity as training progresses. Subsequent methods have aimed to mitigate this trade-off.

CustomDiffusion [12] constrains updates to the text-image cross-attention layers and regularizes training using retrieved class-specific images. Perfusion [32], inspired by ROME [18], applies a gated rank-one update to the key and value projection matrices, anchoring the key space within the subject's super-category to curb overfitting. DBBlend [22] guides generations from an overfit checkpoint by matching the cross-attention maps of an underfit one, adjusting noise levels at each diffusion step accordingly. AttnDB [19] proposes a multi-stage training scheme that learns embedding alignment, attention maps, and subject identity separately, enhancing both identity preservation and prompt fidelity.

Another line of research explores encoder-based meth-

ods [5, 9, 11, 17, 29, 34, 36], which avoid subject-specific fine-tuning and model-specific weight storage. While some of these methods [9, 11, 29, 34] are domain-specific (e.g., human faces or pets) and may still involve limited fine-tuning, others [5, 14] strive for more general-purpose, zero-shot personalization. However, such models often depend on large-scale pretraining involving diffusion models in the loop. In some cases [5], they even rely on supervision from expert-personalized models to construct their training datasets.

In contrast to these encoder-based or architectural modifications, our approach remains firmly grounded in fine-tuning. We leverage the final stages of training to extract and synthesize high-quality images enriched with subject identity cues. These synthesized images are then used to train more efficient personalization models for inference-time deployment. Rather than discarding fine-tuning due to its computational cost, we embrace it as both a powerful personalization mechanism and a source of high-fidelity supervision. Our method is therefore positioned within the fine-tuning paradigm, but repurposed it to enhance prompt adherence and subject alignment while enabling efficient downstream inference—offering a unique balance between quality, adaptability, and efficiency.

3. Method

3.1. Revisiting the Loss Functions Used in Current Personalization Pipelines

Most personalization methods, whether they introduce a new token in the text encoder (*textual inversion* [8]), adapt a small set of weights with low-rank updates (*DreamBooth LoRA* [16, 26]), or fine-tune a lightweight subset of layers (*CustomDiffusion* [12]), often optimize *exactly* the same objective used to train the original diffusion backbone. Given an image x_0 paired with a text prompt τ , Gaussian noise $\epsilon \sim \mathcal{N}(0, \mathbf{I})$ is added according to the forward process, yielding

$$x_t = \sqrt{\bar{\alpha}_t} x_0 + \sqrt{1 - \bar{\alpha}_t} \epsilon$$

The model parameters θ are then updated by minimizing the noise-prediction loss

$$\mathcal{L}_{\text{diff}} = \mathbb{E}_{t, \epsilon, z_0, \tau} [\|\epsilon - \epsilon_\theta(z_t, t, \tau)\|_2^2]$$

This objective treats all pixels equally, regardless of whether they correspond to the object of interest, background, or unrelated regions. Moreover, since it uses a per-pixel L_2 loss, the model is not explicitly encouraged to reconstruct the visual identity of the object; it may converge to solution with low-loss values that perceptually deviate from the reference concept identity.

To address these limitations, we propose two key enhancements: (1) Object-Focused Feature Alignment: We

first localize the object in both the reference and generated images, then extract features specifically from those regions. This enables us to focus the training signal on the object itself, rather than the entire scene. (2) Appearance and Prompt Conditioning: The extracted features disentangle into appearance features (capturing the visual identity) and prompt features (capturing semantic alignment). By supervising the model with both, we explicitly enforce appearance consistency with the reference image while ensuring fidelity to the provided prompt.

3.2. Our approach

Our method is designed to be an easy-to-use add-on on top of existing personalization methods like DreamBooth [26] or Textual-Inversion [8]. It can be applied to a range of base methods and models, from Unet-based diffusion models (e.g SD [25] and SDXL [20]) to DiT-based flow models [15] (e.g FLUX [13] and SD3 [7]). See Figure 2 for an overview of our approach.

In short, our method has two key ideas. First, we start with a specific prompt a specific noise seed. Second, we compute two losses based on the self- and cross- attention features, using a single denoising step of the clean z_0 , and use DIFT [31] to match features between the generated and reference image.

To describe in more detail, we define the following notation. Assume we have a pre-trained (personalized) text-to-image model with tunable parameters θ , and we are given a target prompt p a noise seed z_T , and a reference image x^{ref} of a personalized concept to be learned. The goal is to generate an image based on the prompt that contains the personalized concept. As commonly done, we assume that the target prompt p has a format like "A photo of a [V] [dog] in the park" where [V] denotes the target concept in the prompt. We also assume that the model was already trained with a reference prompt of the form "a photo of [V] [dog]", using some base personalization method like DB-LoRA [16, 26], Textual-Inversion [8], or others [3, 16, 22]. Our method follows four simple steps:

(A) Compute a representation for the reference image:

We compute the latent $z_0^{\text{ref}} = \text{VAE}(x^{\text{ref}})$, then perform a single denoising step of z_0^{ref} , with a denoising parameter α determined with a parameter $t = 1000$. This denoising step is solely for feature extraction and does not change the latent. We then compute two representations of the reference image: (1) appearance features F_0^{ref} of the latent z_0^{ref} from self-attention layers, following the recent PDM method [28]; and (2) cross-attention maps for the concept [V], denoted by M_0^{ref} . For example, in models based on UNet, we took attention maps from all 16 layers of the UNet in Stable Diffusion.

(B) Compute a representation for a generated image:

This follows the same steps like those for reference image. Namely, we first generate a z_0^{gen} using the pretrained model with the prompt p . Then, compute a self attention F_0^{gen} and cross attention features M_0^{gen} for the generated latent z_0^{gen} .

(C) Compute DIFT matching between the two latents

$z_0^{\text{ref}}, z_0^{\text{gen}}$: It gives us a list of n matched pairs of points $(z_0^{\text{ref}}(i), z_0^{\text{gen}}(i)), i = 1, \dots, n$.

(D) Compute three loss components: Using the features extracted as described above, we compute three losses. One based on self-attention, one based on cross-attention, and based on the standard reconstruction loss.

$$\mathcal{L}_{\text{SA}} = \|F_0^{\text{ref}} - F_0^{\text{gen}}\|_{\text{DIFT}} \quad (1)$$

$$\mathcal{L}_{\text{CA}} = \|M_0^{\text{ref}} - M_0^{\text{gen}}\|_{\text{DIFT}} \quad (2)$$

$$\mathcal{L}_{\text{LDM}} = \mathbb{E}_{z_0^{\text{ref}} \sim \mathcal{E}(x^{\text{ref}}), p, \epsilon \sim \mathcal{N}(0, 1), t} \left[\|\epsilon - \epsilon_{\theta}(z_t^{\text{ref}}, t, p)\|_2^2 \right] \quad (3)$$

where the norm $\|\cdot\|_{\text{DIFT}}$ is an L_2 norm taken over the set of matching point pairs computed using DIFT in step C.

Combining all losses gives:

$$\mathcal{L} = \lambda_{\text{SA}} \mathcal{L}_{\text{SA}} + \lambda_{\text{CA}} \mathcal{L}_{\text{CA}} + \lambda_{\text{LDM}} \mathcal{L}_{\text{LDM}} \quad (4)$$

where all λ values are tradeoff coefficients treated as hyperparameters.

Finally, we update the parameters of the personalized model θ using a gradient step over $d\mathcal{L}/d\theta$. The process can be repeated for several gradient steps, but in practice, we found that a single gradient step provided significant improvement.

Richer representations The method described above use only features computed from z_0^{ref} and z_0^{gen} , the cleanest latent. We also explored the case where features are computed from multiple different cleaning steps. For the reference image, this requires inverting the image into z_T^{ref} , and selecting T different denoising steps along the denoising path. For the generated image, we similarly take the corresponding denoising steps along the path. Figure 6 below shows that using more features does improve generation quality, but even $T = 1$ provides a significant benefit.

4. Experiments

This section begins with a description of our implementation setup. We then assess our approach on commonly used benchmarks and show it improves all baselines across different text-to-image diffusion models. Finally, we carry out ablation studies to examine the individual impact of each component in our method.

4.1. Implementation and Evaluation Setup

4.1.1. Implementation Details

Our implementation is based on the publicly available Stable Diffusion V1.5, V2.1 [25], SDXL [20], and FLUX [13] architectures. All experiments are conducted on a single NVIDIA H100 GPU. Both λ_{SA} and $\lambda_{\text{CA}} = 1$ are set to 1. The optimization process of our method takes 4 seconds to tune a personalized model for a specific query. We perform a single optimization step of our method with a batch size of 1 and the same learning rate used during the training procedure of the personalized model.

For the first stage of personalization training (used as a baseline upon which our method builds), we adopted the authors' original implementations and hyperparameters whenever available. While most methods provided public code, we were unable to obtain implementations for DBLend [22], AlignIT [1], and PALP [3]. For these, we re-implemented the algorithms based on the descriptions in their respective papers.

4.1.2. Evaluation Setup

We evaluate our method in two sets of experiments:

(A) On top of six personalization method, including DreamBooth [26], LoRA [16], Textual Invresion [8], DBLend [22], AttnDB [19], and CLD [10]. Results are provided with (w/) and without (w/o) our method across three diffusion models: Stable Diffusion (SD) [25], Stable Diffusion XL (SDXL) [20], and FLUX [13]. For the quantitative evaluation, we follow the literature and evaluate our approach on the DreamBooth's dataset.

(B) Against per-query methods, including AlignIT [1], and PALP [3], on top of different personalization baselines, including Textual Inversion [8], LoRA [16], DB [26], with FLUX [13], SDXL [20], and SD2.1 [25] as backbones. For the quantitative evaluation, we use the TI and CustomConcept101 datasets proposed by [8] and [6], respectively.

4.2. Results

Since our method can be applied on top of existing personalization approaches, we evaluate its benefits by comparing images generated with and without our method.

Specifically, we conducted qualitative and quantitative evaluations between personalization methods [8, 10, 12, 19, 22, 26] with (w/) and without (w/o) our method across FLUX [13], SDXL [20], SD1.5 and SD2.1 [25] backbones. We also provide ablation studies to explore the impact of the components of our method.

4.2.1. Qualitative Evaluation

For evaluation, we used ChatGPT to generate complex prompts that satisfy the following criteria: a prompt was required to contain several elements such as appearance ("as

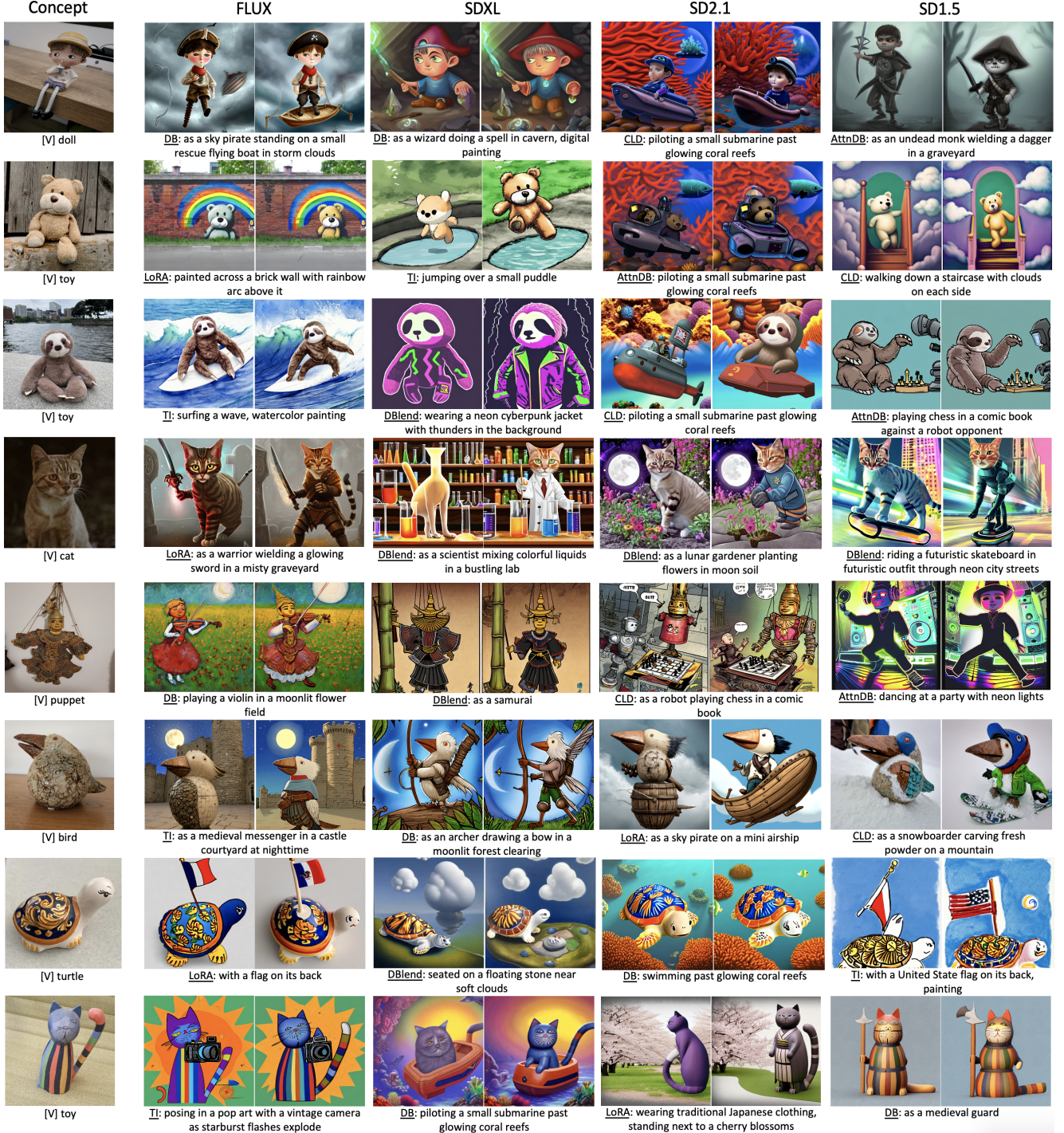


Figure 3. Qualitative comparison. We present images generated by various personalization methods without our method and with it, including DB [26], TI [8], DBblend [22], CLD [10], AttnDB [19], and LoRA [16], across 4 different backbones (FLUX [13], SDXL [20], SD2.1, SD1.5 [25]). The left column shows one example of the target concept, and then every pair of columns shows the generated images with and without our method. Each pair uses the same prompt and seed. Adding our method to those personalization approaches yields better performance in text alignment and identity preservation compared to these baselines. Prompts were generated using ChatGPT.

a wizard”), action (“doing a spell”), scene (“in a cavern”), and style (“digital painting”).

Figure 3 provides a visual comparison of images generated with various state-of-the-art text-to-image personal-

ization methods with (w/) and without (w/o) our method. As observed, for certain queries, without our method, these baselines either: (1) overlooks the learned concept, producing images that solely reflect other prompt tokens (e.g., "puppet as a robot ..."), (2) tends to overfit the new concept, failing to compose it in novel scenes or actions (e.g., "toy surfing ..."), (3) struggle to achieve text-aligned generations (e.g., "doll as a sky pirate ..."), (4) fail to preserve the identity of the learned concept (e.g., "puppet playing a violin ..."). Incorporating our method provides successful text-aligned and identity-preserved personalization for these complex queries. Figure 7 provides a visual comparison between images generated with our method and with two prominent per-query methods (AlignIT [1] and PALP [3]) across different baselines (including DB [26], LoRA [16], TI [8]). Similarly, we observed (1) "puppet sitting ...", (2) "toy dancing ...", (3) "as a Mexican militant ...", (4) "toy as a ringmaster ...", respectively demonstrating the same 4 failure modes noted in the preceding paragraph. Our per-query method, is the only method that successfully generates identity preserved and text-aligned personalized images for these complex prompts. Additional qualitative results can be found in Figures 10 and 11.

4.2.2. Quantitative Evaluation

Following previous work, we quantify the quality of our methods along two key dimensions: (1) Subject Alignment – how well the model preserves the identity of the subject, and (2) Prompt Adherence – how well the model aligns the generated image with the given prompt.

To estimate subject alignment, we use the evaluation benchmark, dataset, and metrics from DreamBooth [26]. We measure the average pairwise cosine similarity between ViT-S/16 CLIP [21] embeddings of generated and real images (denoted as CLIP-I), as well as between ViT-S/16 DINO [4] embeddings (denoted as DINO-I). These metrics provide a proxy for how well the generated images maintain the identity of the original subject.

Prompt adherence is measured using CLIP-T, which calculates the average cosine similarity between the text prompt and the CLIP embedding of the generated image. This evaluates how accurately the generated image reflects the textual description.

Integrating our method into state-of-the-art baselines achieves superior performance on both subject alignment (CLIP-I) and prompt adherence (CLIP-T), as demonstrated in Fig. 4 and 5.

4.3. Ablation Studies and Sensitivity to Parameters

Noise weight: Figure 8 shows using $t = 1000$ when extracting the PDM features and cross-attention maps from z_0 for our loss produces the best performance.

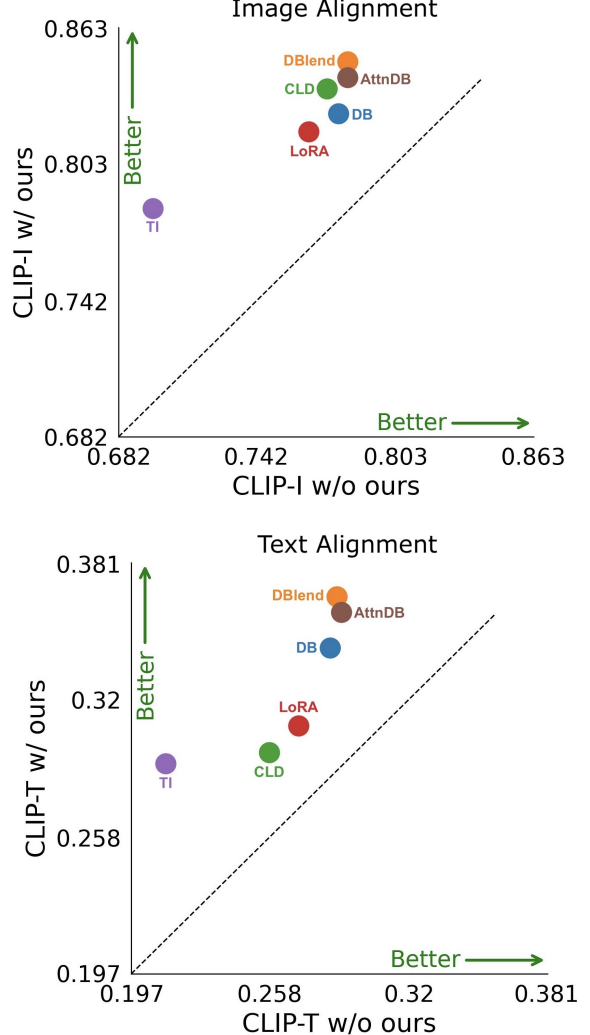


Figure 4. Effect of adding our method to baseline personalization models. Shown are image alignment (top) and text alignment (bottom) of several personalization approaches with (w/) and without (w/o) the integration of our method.

Tuning-time: We describe two sets of experiments designed to reduce the tuning time of our method.

First, shown in Fig. 6, we calculated the loss across different stages of z_t . We found, calculating for the last stage (i.e., z_0) result in sufficient results, while collecting feature from other stages along the denoising path increase the tuning duration.

Second, shown in Fig. 9, we looked into self-attention features from other layers in addition to the last layer used in PDM [28]. The benefit of using more features was negligible, and did not justify the increase in tuning time. Using only the PDM features results in sufficient performance.

Stage-wise loss effectiveness: Shown in Tab. 1, we examined incorporating our proposed losses at other stages as

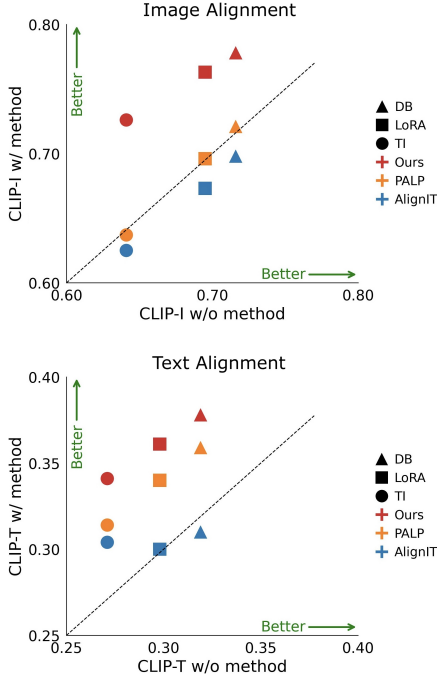


Figure 5. Quantitative Comparison with previous per-query methods. Image alignment (top) and text alignment (bottom) of various personalization approaches (including, DB \blacktriangle , LoRA \blacksquare , and TI \bullet), with (w/) and without (w/o) the integration of different per-query methods (including, AlignIT, PALP, and Ours).

well. Specifically, throughout training, across two prominent

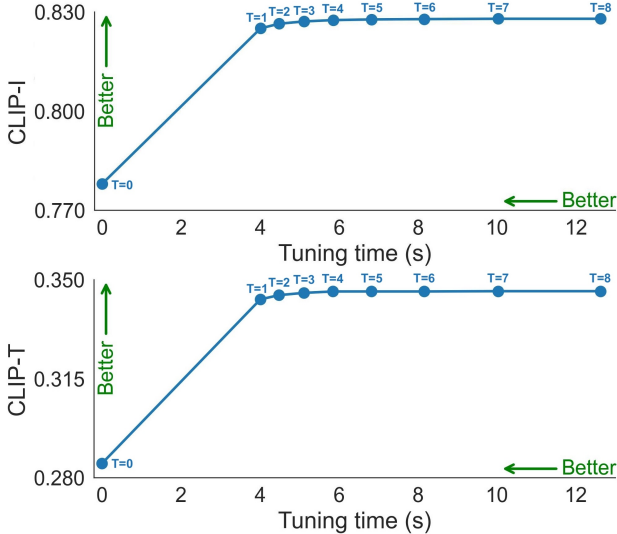


Figure 6. Quality-vs-time tradeoff. Figures show the CLIP-I (top) and CLIP-T (bottom) metrics as a function of fine-tuning duration. The duration is longer when using more features that are collected throughout the denoising path. T is the number of feature maps using to compute the losses.

Method	λ_{PDM}	λ_{CA}	Subject Alignment		Prompt Adherence
			DINO-I \uparrow	CLIP-I \uparrow	CLIP-T \uparrow
DB			0.659 \pm 0.101	0.805 \pm 0.048	0.296 \pm 0.023
DB	✓		0.631 \pm 0.104	0.760 \pm 0.047	0.272 \pm 0.024
DB		✓	0.660 \pm 0.101	0.804 \pm 0.047	0.300 \pm 0.024
TI			0.559 \pm 0.106	0.731 \pm 0.052	0.255 \pm 0.021
TI	✓		0.532 \pm 0.104	0.711 \pm 0.056	0.240 \pm 0.022
TI		✓	0.561 \pm 0.106	0.730 \pm 0.052	0.257 \pm 0.020

Table 1. Stage-wise loss effectiveness ablation study. We examine the effectiveness of \mathcal{L}_{SA} and \mathcal{L}_{CA} throughout training rather than post-training, with two prominent methods, utilizing SD1.5 as backbone, with $\lambda_{PDM} = 1$, $\lambda_{CA} = 1$. We observe inferior results compared to post-training integration, and equal/inferior results compared to the baseline. This quantitatively support that certain losses become effective only after the model reaches a certain state.

ment methods, using SD1.5 [25] as backbone. This ablation quantitatively supports that certain losses become effective only after the model reaches a certain state. Incorporating our objectives throughout training provides inferior results compared to the baseline, while using them post-training provides superior enhancement in terms of subject alignment and prompt adherence.

Method	λ_{PDM}	λ_{CA}	Subject Alignment		Prompt Adherence
			DINO-I \uparrow	CLIP-I \uparrow	CLIP-T \uparrow
DB			0.659 \pm 0.101	0.805 \pm 0.048	0.296 \pm 0.023
DB	✓		0.709 \pm 0.104	0.844 \pm 0.045	0.297 \pm 0.025
DB		✓	0.658 \pm 0.103	0.805 \pm 0.047	0.357 \pm 0.024
DB	✓	✓	0.710 \pm 0.103	0.845 \pm 0.046	0.358 \pm 0.025
TI			0.559 \pm 0.106	0.731 \pm 0.052	0.255 \pm 0.021
TI	✓		0.644 \pm 0.100	0.809 \pm 0.047	0.256 \pm 0.024
TI		✓	0.558 \pm 0.107	0.732 \pm 0.053	0.305 \pm 0.023
TI	✓	✓	0.646 \pm 0.101	0.810 \pm 0.048	0.306 \pm 0.022

Table 2. Per-loss contribution ablation study. We investigate the contribution of each loss in our proposed method. Testing across different methods, leveraging SD1.5 as backbone, and using a fixed $\lambda_{PDM} = 1$, $\lambda_{CA} = 1$ values. \mathcal{L}_{PDM} provides superior subject alignment, and \mathcal{L}_{CA} results superior prompt-adherence. Incorporating both provides superior results in both aspects.

Per-loss contribution: We quantify the contribution of each loss in our proposed method, by incorporating losses separately and together across different methods, using SD1.5 [25] as the backbone, while fixing $\lambda_{SA} = 1$, $\lambda_{CA} = 1$. Tab. 2 shows that \mathcal{L}_{SA} provided superior subject alignment, and \mathcal{L}_{CA} resulted superior prompt-adherence. Incorporating both provided superior results in both aspects.

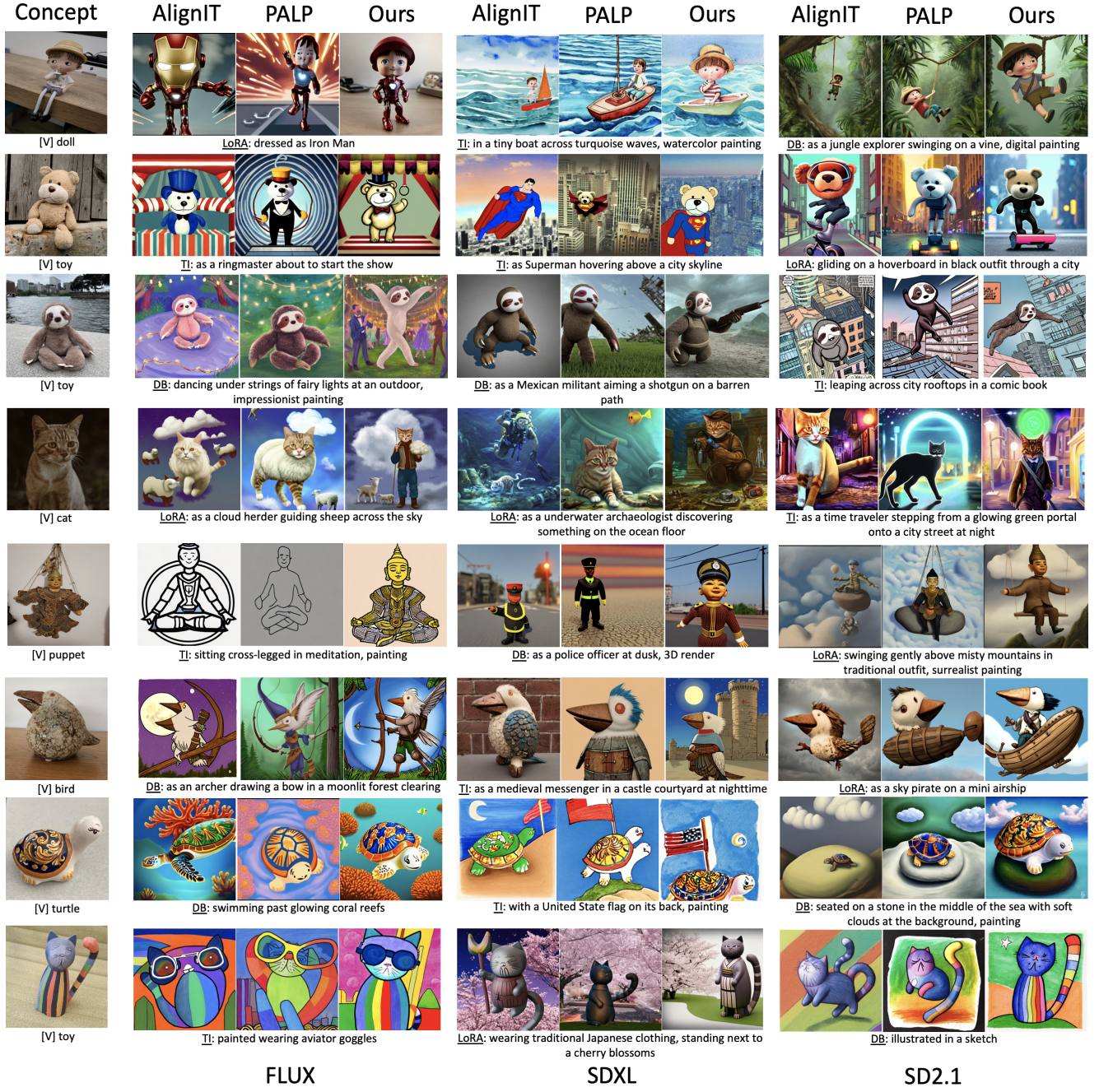


Figure 7. Qualitative comparison. We present images generated by 3 personalization methods (including DB [26], TI [8], LoRA [16]) using 3 per-query methods (including AlignIT [1], PALP [3], Ours), across 3 different backbones (FLUX [13], SDXL [20], SD2.1 [25]). Our method demonstrates superior performance in text alignment and identity preservation compared to these per-query methods. Our per-query method, is the only method that successfully generates identity preserved and text-aligned personalized images for these complex queries.

5. Acknowledgements

This study was funded by the Israeli Ministry of Science, Israel-Singapore binational grant, and by a grant from the Israeli higher-council of education, through the Bar-Ilan data science institute (BIU DSI).

References

[1] Aishwarya Agarwal, Srikrishna Karanam, and Balaji Vasan Srinivasan. Alignit: Enhancing prompt alignment in customization of text-to-image models. In *2025 IEEE/CVF Winter Conference on Applications of Computer Vision (WACV)*, pages 4882–4890. IEEE, 2025. [2](#), [4](#), [6](#), [8](#), [12](#)

[2] Yuval Alaluf, Elad Richardson, Gal Metzer, and Daniel Cohen-Or. A neural space-time representation for text-to-image personalization. *arXiv preprint arXiv:2305.15391*, 2023. [2](#)

[3] Moab Arar, Andrey Voynov, Amir Hertz, Omri Avrahami, Shlomi Fruchter, Yael Pritch, Daniel Cohen-Or, and Ariel Shamir. Palp: Prompt aligned personalization of text-to-image models. *arXiv preprint arXiv:2401.06105*, 2024. [2](#), [3](#), [4](#), [6](#), [8](#), [12](#)

[4] Mathilde Caron, Hugo Touvron, Ishan Misra, Hervé Jégou, Julien Mairal, Piotr Bojanowski, and Armand Joulin. Emerging properties in self-supervised vision transformers. In *Proceedings of the IEEE/CVF international conference on computer vision*, pages 9650–9660, 2021. [6](#)

[5] Wenhui Chen, Hexiang Hu, Yandong Li, Nataniel Ruiz, Xuhui Jia, Ming-Wei Chang, and William W Cohen. Subject-driven text-to-image generation via apprenticeship learning. *Advances in Neural Information Processing Systems*, 36:30286–30305, 2023. [3](#)

[6] Jooyoung Choi, Yunjey Choi, Yunji Kim, Junho Kim, and Sungroh Yoon. Custom-edit: Text-guided image editing with customized diffusion models. *arXiv preprint arXiv:2305.15779*, 2023. [4](#)

[7] Patrick Esser, Sumith Kulal, Andreas Blattmann, Rahim Entezari, Jonas Müller, Harry Saini, Yam Levi, Dominik Lorenz, Axel Sauer, Frederic Boesel, et al. Scaling rectified flow transformers for high-resolution image synthesis. In *Forty-first international conference on machine learning*, 2024. [3](#)

[8] Rinon Gal, Yuval Alaluf, Yuval Atzmon, Or Patashnik, Amit H Bermano, Gal Chechik, and Daniel Cohen-Or. An image is worth one word: Personalizing text-to-image generation using textual inversion. *arXiv preprint arXiv:2208.01618*, 2022. [1](#), [2](#), [3](#), [4](#), [5](#), [6](#), [8](#), [12](#)

[9] Rinon Gal, Moab Arar, Yuval Atzmon, Amit H Bermano, Gal Chechik, and Daniel Cohen-Or. Encoder-based domain tuning for fast personalization of text-to-image models. *ACM Transactions on Graphics (TOG)*, 42(4):1–13, 2023. [3](#)

[10] Jiannan Huang, Jun Hao Liew, Hanshu Yan, Yuyang Yin, Yao Zhao, Humphrey Shi, and Yunchao Wei. Classdiffusion: More aligned personalization tuning with explicit class guidance. *arXiv preprint arXiv:2405.17532*, 2024. [4](#), [5](#), [12](#)

[11] Xuhui Jia, Yang Zhao, Kelvin CK Chan, Yandong Li, Han Zhang, Boqing Gong, Tingbo Hou, Huisheng Wang, and Yu-Chuan Su. Taming encoder for zero fine-tuning image customization with text-to-image diffusion models. *arXiv preprint arXiv:2304.02642*, 2023. [3](#)

[12] Nupur Kumari, Bingliang Zhang, Richard Zhang, Eli Shechtman, and Jun-Yan Zhu. Multi-concept customization of text-to-image diffusion. In *Proceedings of the IEEE/CVF conference on computer vision and pattern recognition*, pages 1931–1941, 2023. [2](#), [3](#), [4](#)

[13] Black Forest Labs, Stephen Batifol, Andreas Blattmann, Frederic Boesel, Saksham Consul, Cyril Diagne, Tim Dockhorn, Jack English, Zion English, Patrick Esser, Sumith Kulal, Kyle Lacey, Yam Levi, Cheng Li, Dominik Lorenz, Jonas Müller, Dustin Podell, Robin Rombach, Harry Saini, Axel Sauer, and Luke Smith. Flux.1 kontext: Flow matching for in-context image generation and editing in latent space, 2025. [1](#), [2](#), [3](#), [4](#), [5](#), [8](#), [12](#)

[14] Dongxu Li, Junnan Li, and Steven Hoi. Blip-diffusion: Pre-trained subject representation for controllable text-to-image generation and editing. *Advances in Neural Information Processing Systems*, 36:30146–30166, 2023. [3](#)

[15] Yaron Lipman, Ricky TQ Chen, Heli Ben-Hamu, Maximilian Nickel, and Matt Le. Flow matching for generative modeling. *arXiv preprint arXiv:2210.02747*, 2022. [3](#)

[16] LoRA. Low-rank adaptation for fast text-to-image diffusion fine-tuning. <https://github.com/cloneofsimo/lora>, 2022. [1](#), [2](#), [3](#), [4](#), [5](#), [6](#), [8](#), [12](#)

[17] Yiyang Ma, Huan Yang, Wenjing Wang, Jianlong Fu, and Jiaying Liu. Unified multi-modal latent diffusion for joint subject and text conditional image generation. *arXiv preprint arXiv:2303.09319*, 2023. [3](#)

[18] Kevin Meng, David Bau, Alex Andonian, and Yonatan Beilinkov. Locating and editing factual associations in gpt. *Advances in neural information processing systems*, 35:17359–17372, 2022. [2](#)

[19] Lianyu Pang, Jian Yin, Baoquan Zhao, Feize Wu, Fu Lee Wang, Qing Li, and Xudong Mao. Attndreambooth: Towards text-aligned personalized text-to-image generation. *Advances in Neural Information Processing Systems*, 37:39869–39900, 2024. [2](#), [4](#), [5](#), [12](#)

[20] Dustin Podell, Zion English, Kyle Lacey, Andreas Blattmann, Tim Dockhorn, Jonas Müller, Joe Penna, and Robin Rombach. Sdxl: Improving latent diffusion models for high-resolution image synthesis. *arXiv preprint arXiv:2307.01952*, 2023. [1](#), [2](#), [3](#), [4](#), [5](#), [8](#), [12](#)

[21] Alec Radford, Jong Wook Kim, Chris Hallacy, Aditya Ramesh, Gabriel Goh, Sandhini Agarwal, Girish Sastry, Amanda Askell, Pamela Mishkin, Jack Clark, et al. Learning transferable visual models from natural language supervision. In *International conference on machine learning*, pages 8748–8763. PMLR, 2021. [6](#)

[22] Shwetha Ram, Tal Neiman, Qianli Feng, Andrew Stuart, Son Tran, and Trishul Chilimbi. Dreamblend: Advancing personalized fine-tuning of text-to-image diffusion models. 2025. [1](#), [2](#), [3](#), [4](#), [5](#), [12](#)

[23] Aditya Ramesh, Mikhail Pavlov, Gabriel Goh, Scott Gray, Chelsea Voss, Alec Radford, Mark Chen, and Ilya Sutskever. Zero-shot text-to-image generation. In *International conference on machine learning*, pages 8821–8831. Pmlr, 2021. [2](#)

[24] Aditya Ramesh, Prafulla Dhariwal, Alex Nichol, Casey Chu, and Mark Chen. Hierarchical text-conditional image generation with clip latents. *arXiv preprint arXiv:2204.06125*, 1(2):3, 2022.

[25] Robin Rombach, Andreas Blattmann, Dominik Lorenz, Patrick Esser, and Björn Ommer. High-resolution image synthesis with latent diffusion models. In *Proceedings of the IEEE/CVF conference on computer vision and pattern recognition*, pages 10684–10695, 2022. 1, 2, 3, 4, 5, 7, 8, 12

[26] Nataniel Ruiz, Yuanzhen Li, Varun Jampani, Yael Pritch, Michael Rubinstein, and Kfir Aberman. Dreambooth: Fine tuning text-to-image diffusion models for subject-driven generation. In *Proceedings of the IEEE/CVF conference on computer vision and pattern recognition*, pages 22500–22510, 2023. 1, 2, 3, 4, 5, 6, 8, 12

[27] Chitwan Saharia, William Chan, Saurabh Saxena, Lala Li, Jay Whang, Emily L Denton, Kamyar Ghasemipour, Raphael Gontijo Lopes, Burcu Karagol Ayan, Tim Salimans, et al. Photorealistic text-to-image diffusion models with deep language understanding. *Advances in neural information processing systems*, 35:36479–36494, 2022. 2

[28] Dvir Samuel, Rami Ben-Ari, Matan Levy, Nir Darshan, and Gal Chechik. Where’s waldo: Diffusion features for personalized segmentation and retrieval. *Advances in Neural Information Processing Systems*, 37:128160–128181, 2024. 2, 3, 6

[29] Jing Shi, Wei Xiong, Zhe Lin, and Hyun Joon Jung. Instantbooth: Personalized text-to-image generation without test-time finetuning. In *Proceedings of the IEEE/CVF conference on computer vision and pattern recognition*, pages 8543–8552, 2024. 3

[30] Quan Sun, Qiyi Yu, Yufeng Cui, Fan Zhang, Xiaosong Zhang, Yueze Wang, Hongcheng Gao, Jingjing Liu, Tiejun Huang, and Xinlong Wang. Emu: Generative pretraining in multimodality. *arXiv preprint arXiv:2307.05222*, 2023. 2

[31] Luming Tang, Menglin Jia, Qianqian Wang, Cheng Perng Phoo, and Bharath Hariharan. Emergent correspondence from image diffusion. In *NeurIPS*, 2023. 3

[32] Yoad Tewel, Rinon Gal, Gal Chechik, and Yuval Atzmon. Key-locked rank one editing for text-to-image personalization. In *ACM SIGGRAPH 2023 conference proceedings*, pages 1–11, 2023. 2

[33] Andrey Voynov, Qinghao Chu, Daniel Cohen-Or, and Kfir Aberman. p+: Extended textual conditioning in text-to-image generation. *arXiv preprint arXiv:2303.09522*, 2023. 2

[34] Qixun Wang, Xu Bai, Haofan Wang, Zekui Qin, Anthony Chen, Huaxia Li, Xu Tang, and Yao Hu. Instantid: Zero-shot identity-preserving generation in seconds. *arXiv preprint arXiv:2401.07519*, 2024. 3

[35] Yuxiang Wei, Yabo Zhang, Zhilong Ji, Jinfeng Bai, Lei Zhang, and Wangmeng Zuo. Elite: Encoding visual concepts into textual embeddings for customized text-to-image generation. In *Proceedings of the IEEE/CVF International Conference on Computer Vision*, pages 15943–15953, 2023. 2

[36] Hu Ye, Jun Zhang, Sibo Liu, Xiao Han, and Wei Yang. Ip-adapter: Text compatible image prompt adapter for text-to-image diffusion models. *arXiv preprint arXiv:2308.06721*, 2023. 3

[37] Jiahui Yu, Yuanzhong Xu, Jing Yu Koh, Thang Luong, Gunnar Baid, Zirui Wang, Vijay Vasudevan, Alexander Ku, Yinfei Yang, Burcu Karagol Ayan, et al. Scaling autoregressive models for content-rich text-to-image generation. *arXiv preprint arXiv:2206.10789*, 2(3):5, 2022. 2

[38] Xulu Zhang, Xiaoyong Wei, Wentao Hu, Jinlin Wu, Jiaxin Wu, Wengyu Zhang, Zhaoxiang Zhang, Zhen Lei, and Qing Li. A survey on personalized content synthesis with diffusion models. *arXiv preprint arXiv:2405.05538*, 2024. 1

A. Additional qualitative results

We present additional qualitative comparisons, showcasing results with and without our method applied to various personalization techniques (Figure 10), as well as comparisons against other per-query methods (Figure 11). These figures highlight that our approach significantly enhances generation quality by improving both image alignment (better visual consistency with the reference image) and text alignment (more faithful adherence to the prompt).

B. Ablation Study

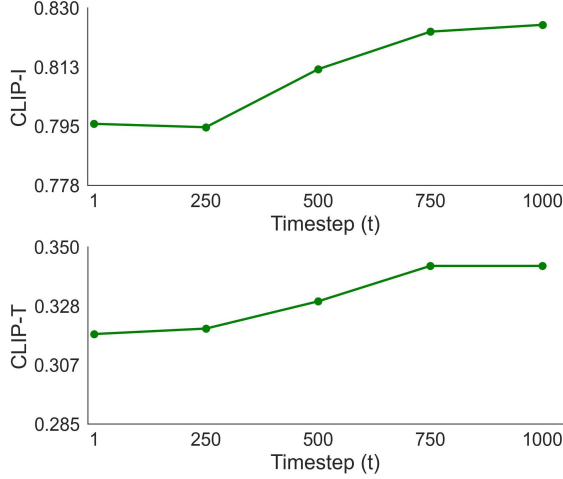


Figure 8. Noise weight Ablation Study. Sensitivity of CLIP-I and CLIP-T metrics to the magnitude of the noise, in terms of the t parameter used when calculating features.

Section 3 describes the feature extraction process. In the main paper, we use a fixed value of $t = 1000$. Here, we explore how varying t affects the results. Figure 8 presents CLIP-I and CLIP-T scores across different t values on the DreamBooth dataset. The results indicate that $t = 1000$ consistently yields the best performance.

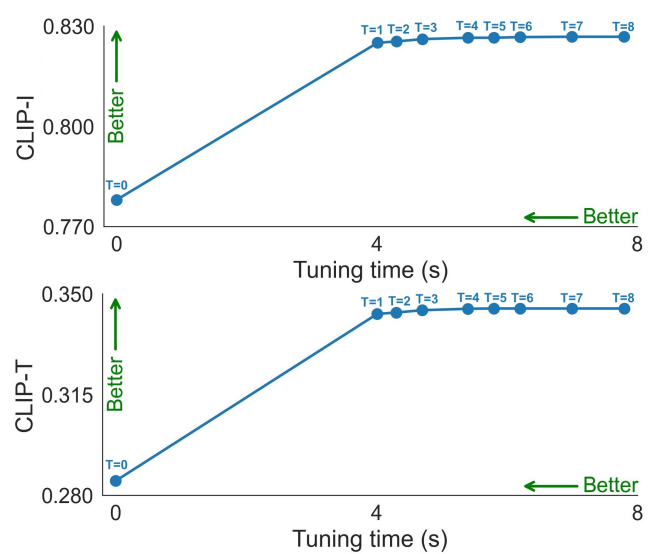


Figure 9. Quality-vs-time tradeoff. Figures show the CLIP-I (top) and CLIP-T (bottom) metrics as a function of fine-tuning duration. The duration is longer when using more SA features that are collected throughout the denoising path. T is the number of feature maps using to compute the losses.

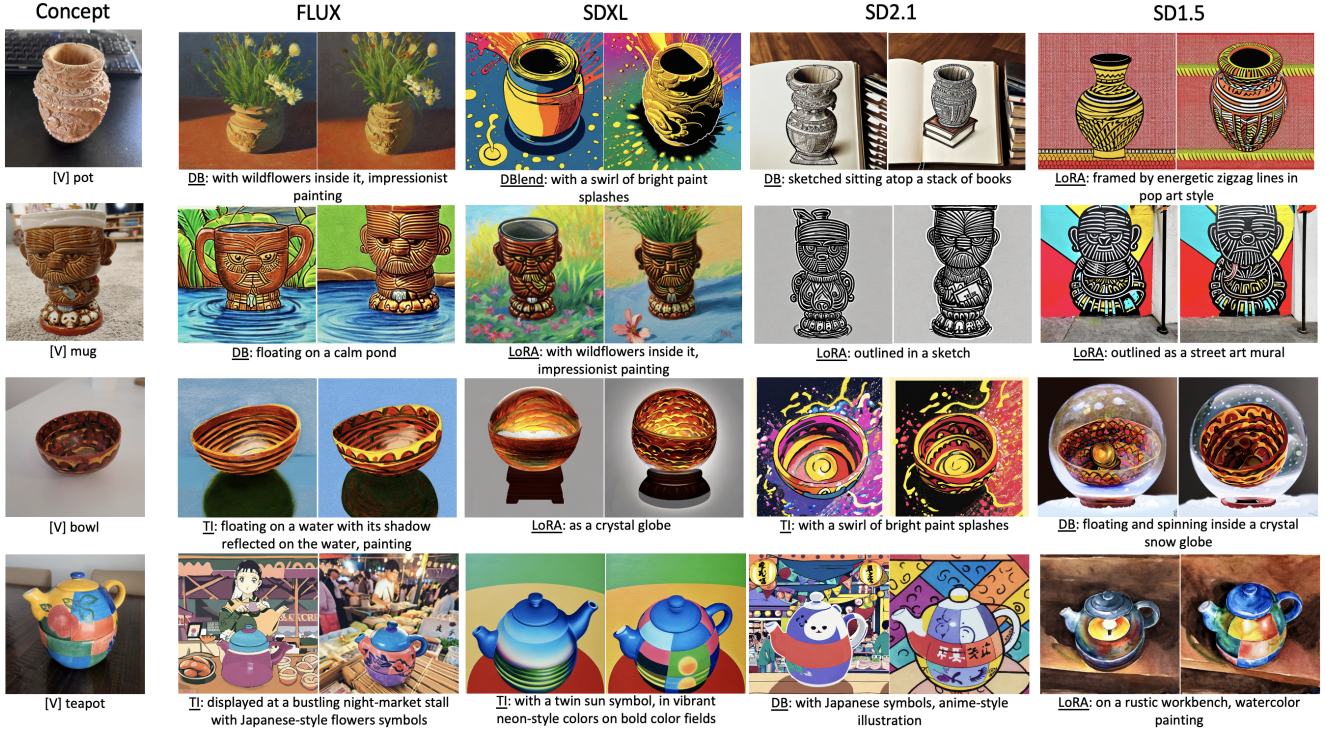


Figure 10. Additional qualitative comparison. We present images generated by various personalization methods without our method and with it, including DB [26], TI [8], DBblend [22], CLD [10], AttnDB [19], and LoRA [16], across 4 different backbones (FLUX [13], SDXL [20], SD2.1, SD1.5 [25]). Adding our method to those personalization approaches demonstrates superior performance in text alignment and identity preservation compared to these baselines.

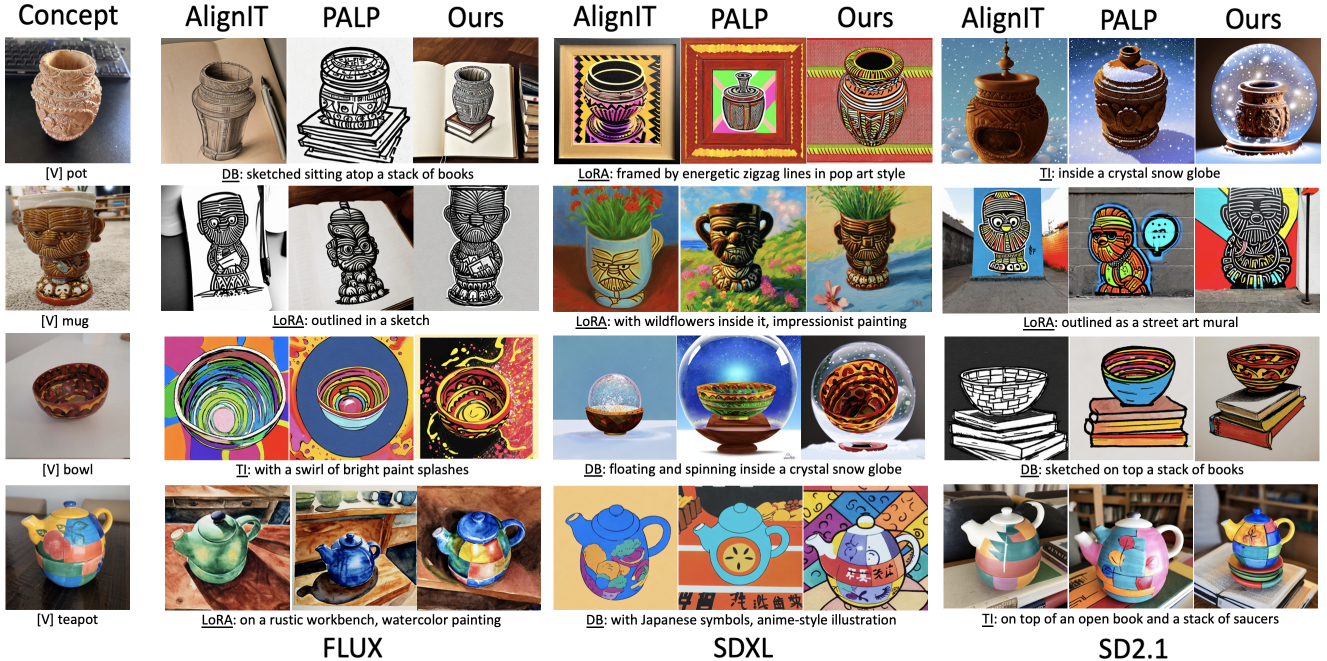


Figure 11. Additional qualitative comparison. We present images generated by 3 personalization methods (including DB [26], TI [8], LoRA [16]) using 3 per-query methods (including AlignIT [1], PALP [3], Ours), across 3 different backbones (FLUX [13], SDXL [20], SD2.1 [25]). Our method demonstrates superior performance in text alignment and identity preservation compared to these per-query methods.